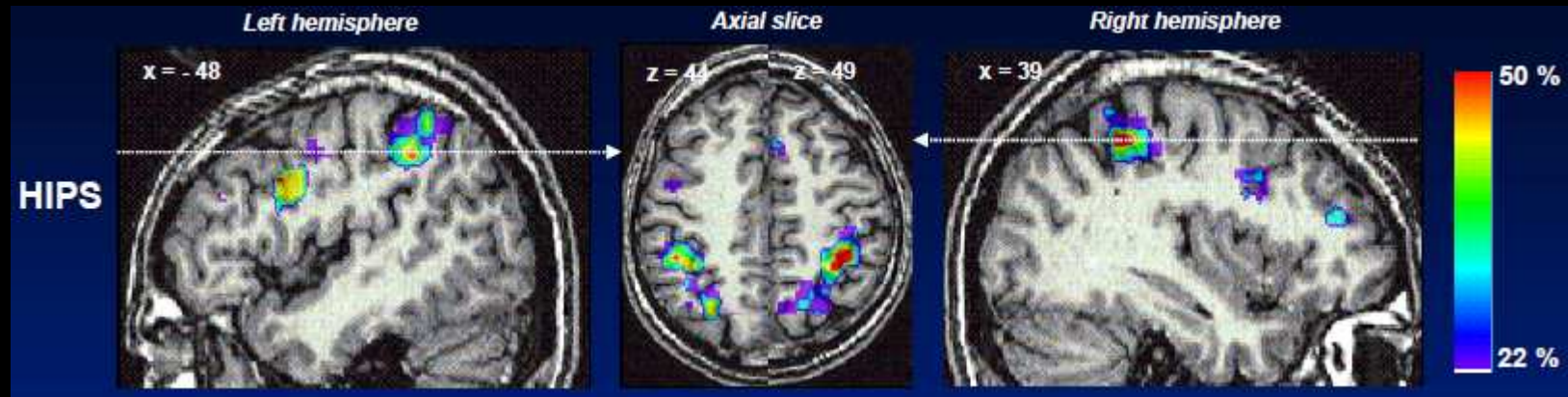


***An exploratory study  
Of EEG synchrony during  
mental calculations***

Dimitriadis Stavros  
Master Thesis  
AIIA - 2010



# The number sense and the horizontal segment of the intraparietal sulcus (HIPS)

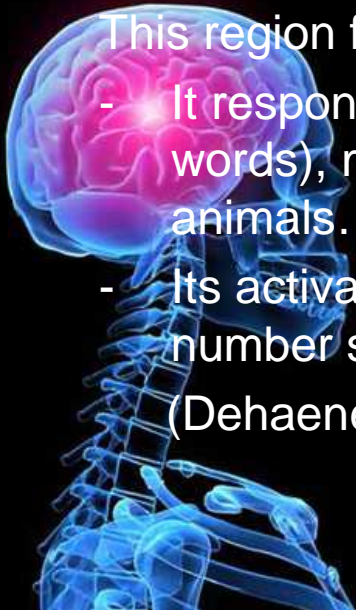


- All numerical tasks activate this region (e.g. addition, subtraction, comparison, approximation, digit detection,..)

This region fulfills two criteria for a semantic – level representation:

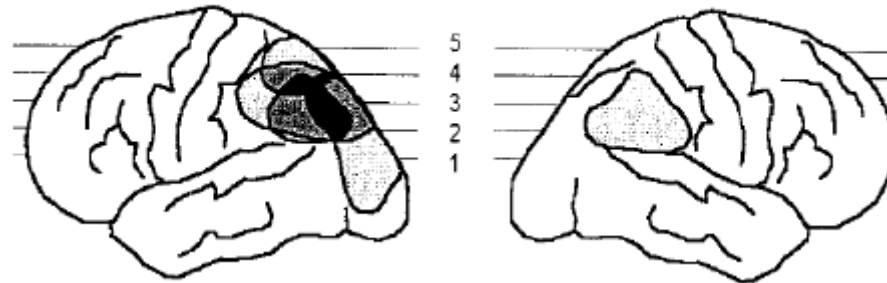
- It responds to number in various formats (Arabic digits, written and spoken words), more than to other categories of objects (e.g. letters, colors, animals...)
- Its activation varies according to a semantic metric (numerical distance, number size)

(Dehaene et al., 2003)

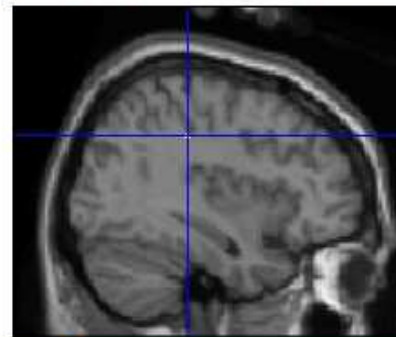
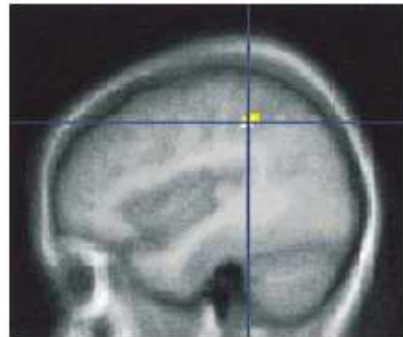


# Parietal dysfunction causes impairments in number sense

Lesions causing acalculia in adults



Anomalies correlated with developmental dyscalculia in children



**Dyscalculic adults born pre-term** show missing gray matter in the intraparietal sulcus, compared to non-dyscalculic pre-term controls. (Isaacs et al., 2001)

**Turner's syndrome** (monosomy 45-X) is frequently associated with dyscalculia. We found that a group of Turners girls showed both structural and functional alterations in the intraparietal sulcus (Molko et al., 2003)





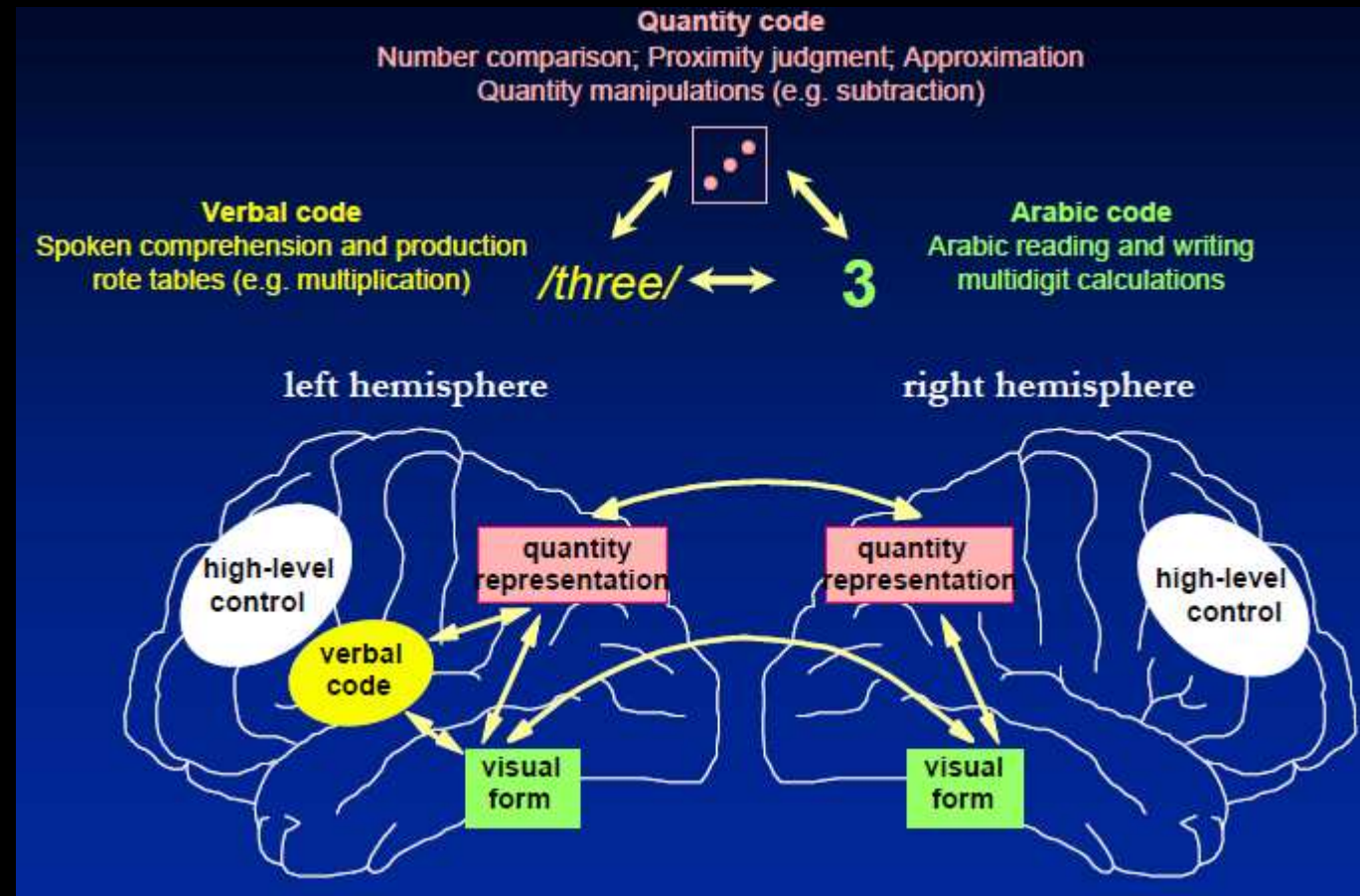


# Does human IPS contain number neurons ?

- Two recent studies suggest that while quantity adaptation in the left IPS is independent of stimulus format, the right IPS only adapts to quantity when represented by Arabic numerals.
- Left IPS specialized for symbolic, enculturated representations of quantity (e.g. Arabic numerals and number words) that may be afforded by connections with left – frontal language related regions of the brain.  
(Cohen Kadosh et al., 2007 and Piazza et al., 2007)
- Damage to left parietal regions has consistently been associated with calculation deficits (Dehaene and Cohen, 1995).
- In summary, the studies from (Cohen Kadosh et al., 2007 and Piazza et al., 2007) reveal the possibility of both format-dependent and abstract processing of number in the IPS.



# Attaching symbols to quantities: The triple – code model of number processing

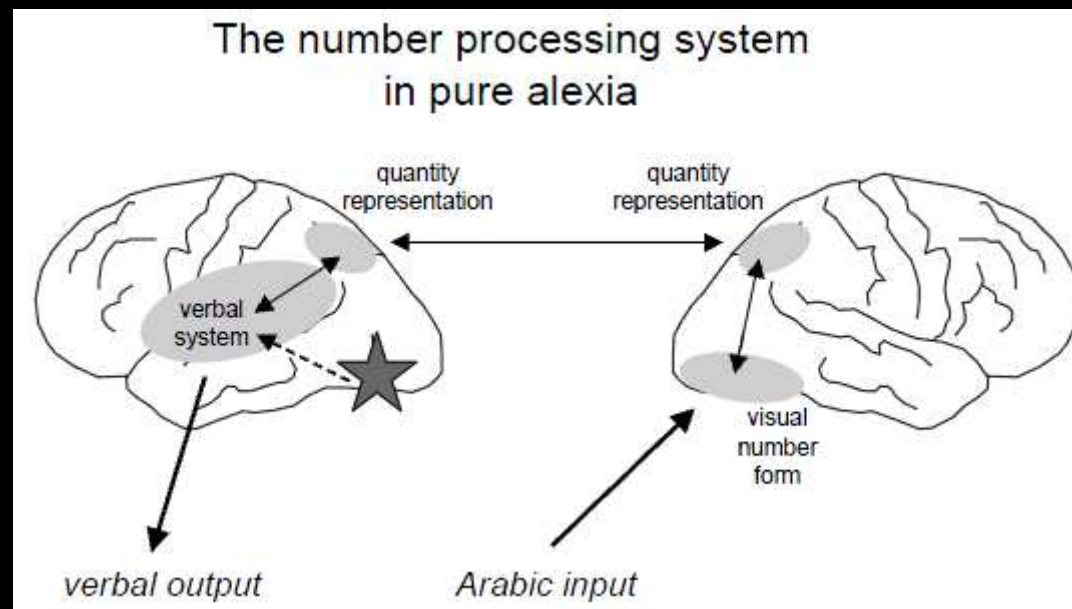


(Dehaene et al., 2003)



# Arithmetic calculations in pure alexic

- Anatomical and functional model of the number processing system as lesioned in pure alexia. Arabic numerals and abstract quantities can be processed by both hemispheres, while only the left hemisphere is able to represent numbers in a verbal format. Pure alexia for numbers results from an impairment of the left hemispheric visual number form, precluding the translation of arabic numerals into words, and hence the retrieval of stored multiplication facts. Subtraction problems can still be solved, like number comparison, on the basis of the quantity representation.



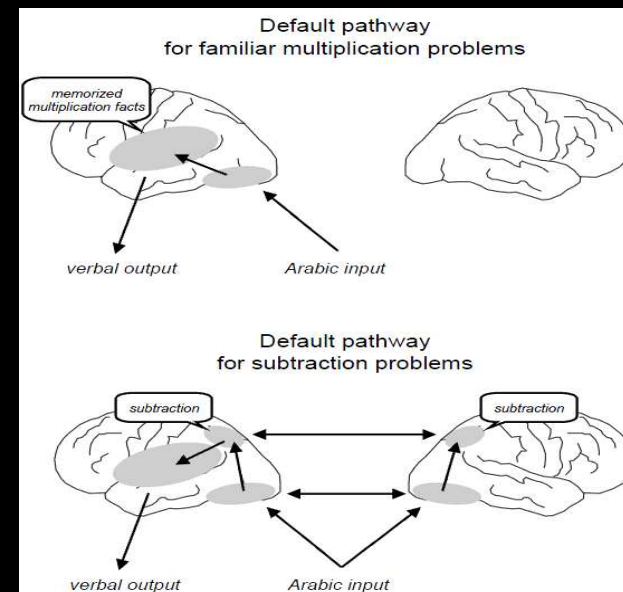
(Cohen and Dehaene, 1995)





# Arithmetic calculations in pure alexic

- Default pathways thought to be used for solving familiar multiplication problems (*upper panel*), and subtraction problems (*lower panel*). Multiplication facts are learned by rote and retrieved as automatic verbal associations. Subtraction requires the manipulation of the quantities represented by the operands.
- There must be two distinct visual identification processes for numbers, one that is the mandatory input pathway to naming and multiplication processes, and the other that is able to supply comparison, addition, subtraction and simple division routines. Only the first of these seems to be impaired in single studies in pure alexic patients.

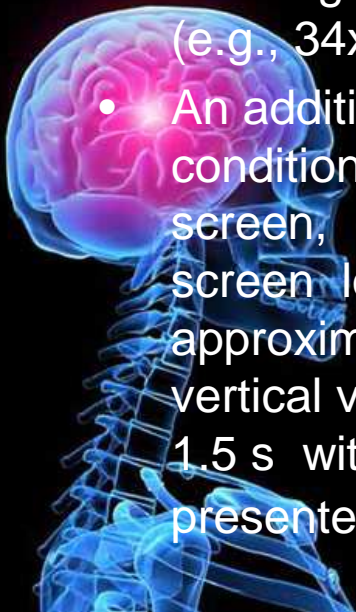


(Cohen and Dehaene, 1995)



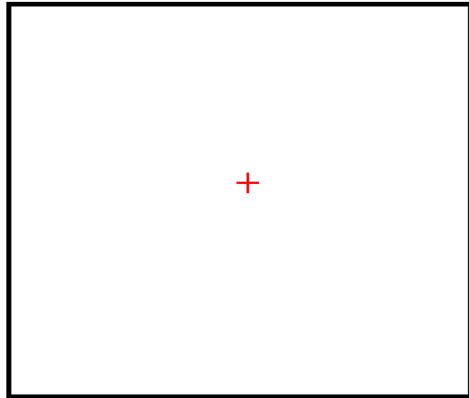
## Current dataset

- The present study concerned 18 right-handed volunteers (aged: 21–26 years, mean 23 years, who were Medical School students in the University of Crete) during performance of arithmetic tasks differing in nature and level of complexity.
- Continuous EEG was recorded while subjects were performing either of the two arithmetic tasks: (1) Four-digit number comparison (e.g., 5467 versus 6689; numbers in “different pairs” differed by less than 20%). The position of the larger number varied randomly, and participants had to raise their left index finger if the number on top was greater and their right finger if the lower was greater; (2) Two-digit multiplication (e.g.,  $34 \times 23$ ,  $49 \times 32$ ).
- An additional Baseline EEG was recorded during a passive viewing condition (i.e. participants simply fixated at the centre of the computer screen, on a small red cross). Stimuli were presented on an LCD screen located in front of the participants at a distance of approximately 80 cm, subtending  $2-3^\circ$  and  $2-4^\circ$  of horizontal and vertical visual angle, respectively. Stimulus presentation was always for 1.5 s with an ISI of 0.5 s, during which a fixation star was presented.



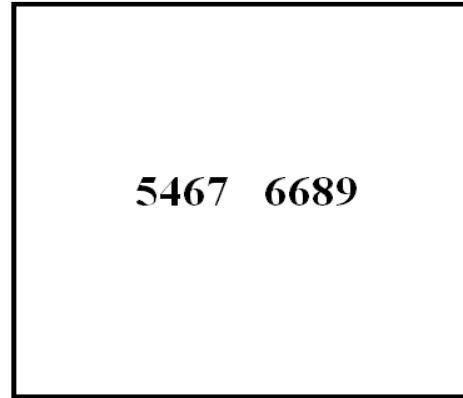
# Schematic illustration of the three conditions

a)



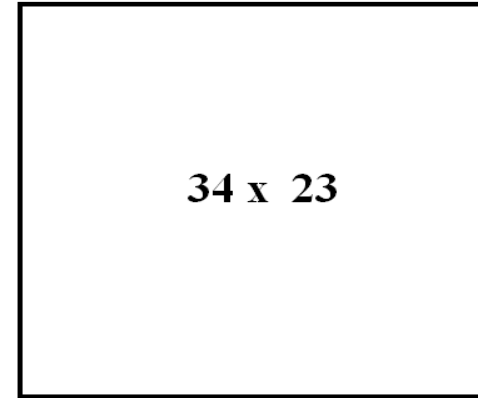
**Control**

b)



**Comparison**

c)

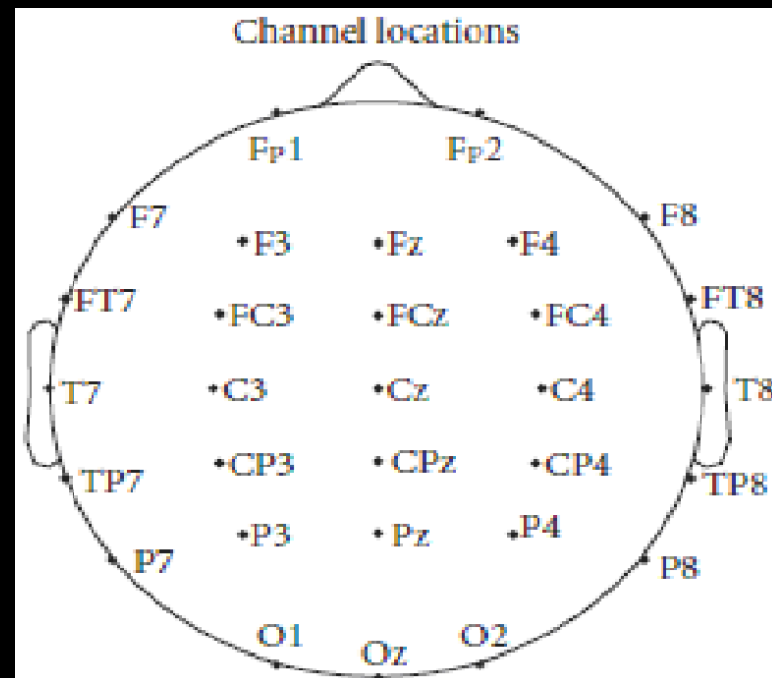


**Multiplication**



# EEG recordings

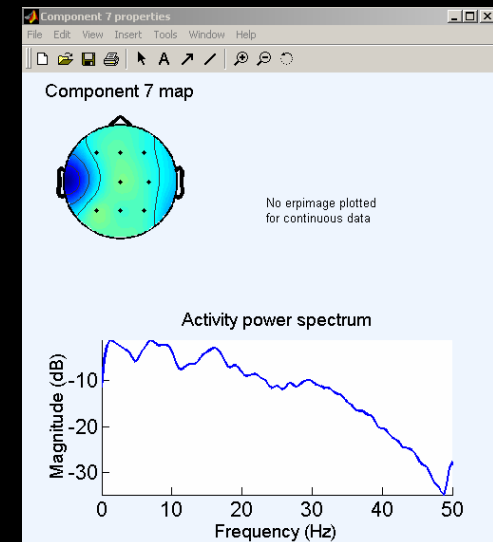
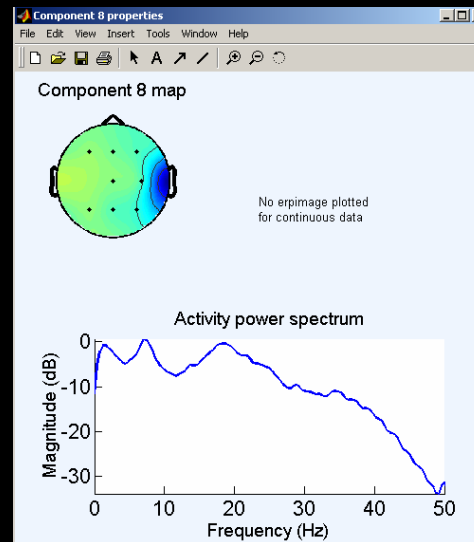
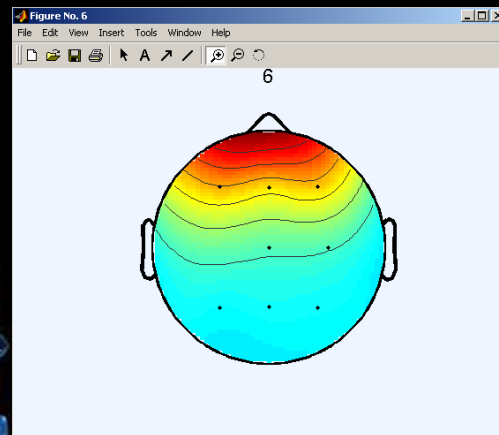
- The EEG was recorded from 30 electrodes according to the international 10/20 system:FP2, F4, FC4, C4, CP4, P4, O2, F8, FT8, T4, TP8, PO8, Fz, FCz, Cz, CPz, Pz, Oz, FP1, F3, FC3, C3, CP3, P3, O1, F7, FT7, T3, TP7, PO7, and A1 + A2 as reference).
- Vertical and horizontal eye movements and blinks were monitored through a bipolar montage from the supraorbital ridge and the lateral canthus.





# Preprocessing steps

- The signals were amplified using a set of Contact Precision Instrument amplifier, filtered online with a (0.1-200) Hz band pass and digitized at 500 Hz.
- Artifact-free epochs of 8 s were selected, via visual inspection, from each subject and for each recording condition.
- Applying ICA (Delorme and Makeig, 2004), we verified that there were no signal components that could be associated with artifactual activity from eyes or muscles.



- Using a zero phase pass-band filter, the multichannel EEG-signal was split into 5 different bands, which are traditionally defined and denoted as follows:  $\theta$  (4-8 Hz),  $\alpha_1$  (8-10 Hz),  $\alpha_2$  (10-13 Hz),  $\beta$  (13-30 Hz), and  $\gamma$  (30-45 Hz).

# Contrast function

Two different sets of multidimensional patterns/objects  $\{X_i\}$  and  $\{Y_j\}$  can be compared in three steps. We first establish an appropriate pairwise dissimilarity measure  $D(X_i, Y_j)$ . This measure is then applied to all possible pairs in order to compute an inter-set scatter (IS) and the two within-set scatters (WS). Finally, the computed quantities are combined appropriately to express the set-difference as follows:

$$J = J(\{X_i\}, \{Y_j\}) = \frac{IS_{control \leftrightarrow active}}{WS_{control} + WS_{active}} = \frac{1}{2} \frac{\sum_{i=1}^N \sum_{j=1}^N D(X_i, Y_j)}{\sum_{i=1}^N \sum_{j>i}^N D(X_i, X_j) + \sum_{i=1}^N \sum_{j>i}^N D(Y_i, Y_j)}$$

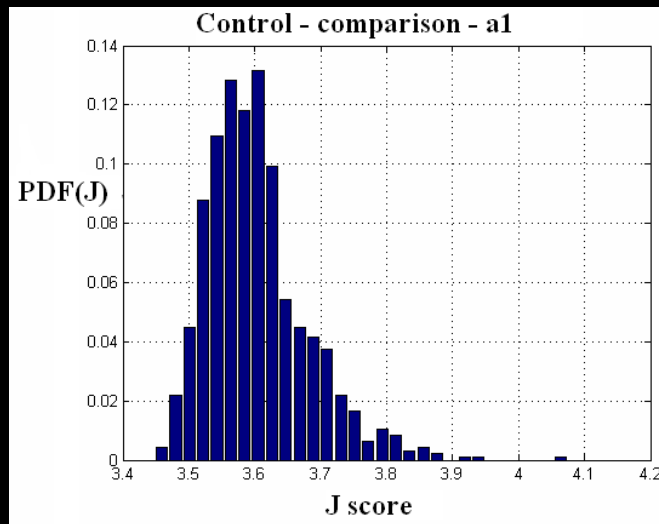
The contrast-function measures the class separability, with the J-index taking the value of 1 when classes are highly overlapped and growing monotonically as classes are getting more distinguishable.

$D$  = (Euclidean distance, Frobenius norm, VI distance)



# Statistical significance of J-index

- Statistical significance of J-index can be calculated based on a randomization procedure (Good,2000), which proceeds by splitting the objects, at random, in two groups and repeating the same computations multiple times, in order to form a baseline distribution for the J-index indicative of random partitioning. Finally the original J-value is compared against the emerged baseline distribution, and this comparison is expressed via a P-value.





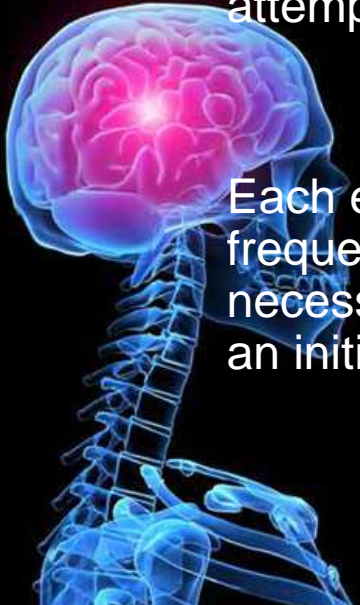
# The different state-representations

## 1. Multisite Signal Power patterns

(30D, 8D (8 lobes) , 2D (2 hemispheres), single electrodes)

## 2. Functional Connectivity Pattern and its Graph representations

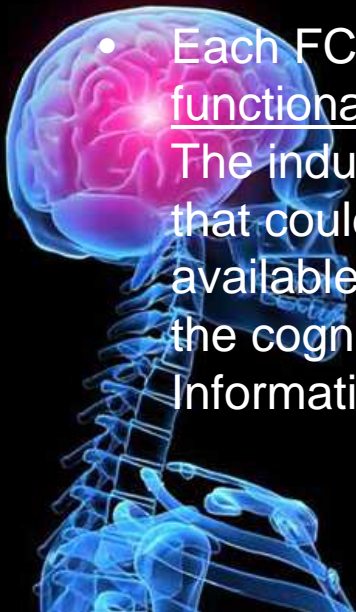
- Coherence (COH) is a linear measure working in the frequency domain and incorporating both amplitude and phase characteristics.
- Quiroga's Nonlinear Interdependence (NI) is a nonlinear measure based on similarities between trajectories of the underlying dynamical systems (Quiroga et al, 2002 ).
- Phase Locking index (PLI) neutralizes the effects of amplitude variation, utilizes Morlet's wavelet transform to estimate instantaneous phases and attempts a statistical aggregation of phase-differences.



Each estimator was applied (using signals filtered within a particular frequency band) to every possible pair of electrodes. Any parameter necessary for the estimators was selected via exhaustive search, during an initial 'training-stage' so as to maximize the contrast function.

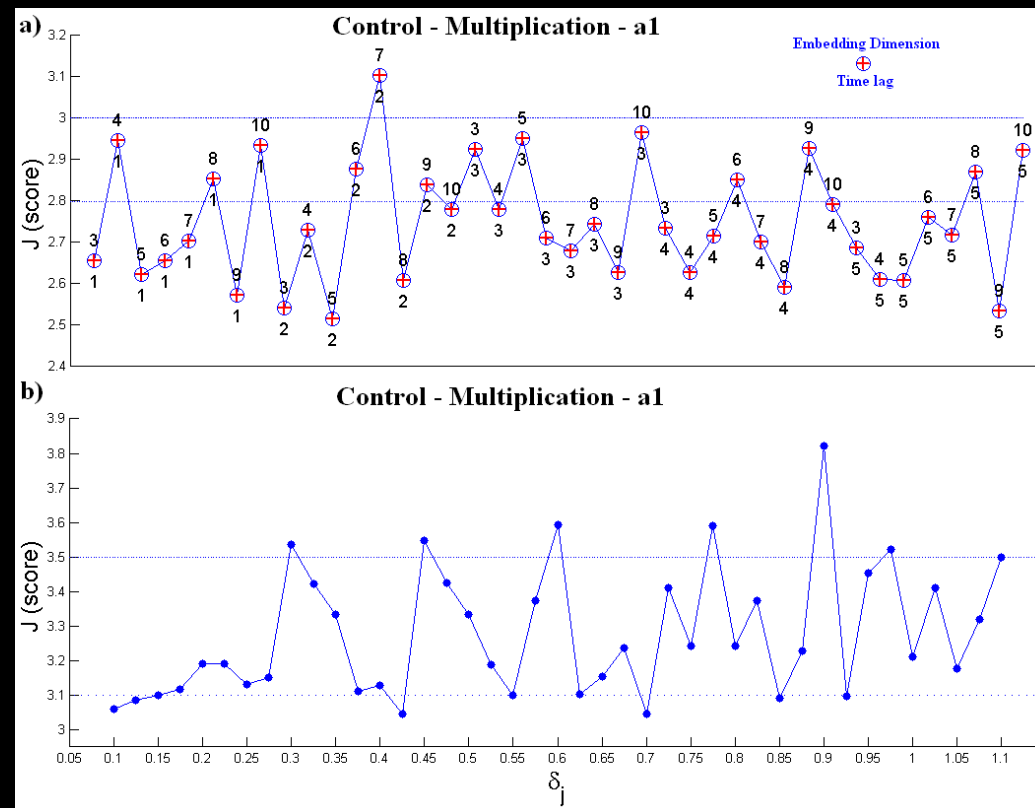
# The different state-representations

- The computed estimates were tabulated in a [30x30] matrix.
- The importance of a lower-resolution description of dynamical interactions was also tested by using FCG resulting from the spatial grouping of electrodes (into Frontal, Temporal, Central, Parieto-Occipital groups symmetrically defined over left and right hemisphere). The entries of these [8 x 8] matrices were deduced from the original [30 x 30] connectivity matrices by summing according to the spatial groups.
- The sets of FCG graphs during control and an active state could be readily compared using our contrast function, by incorporating the *Frobenious norm* as the dissimilarity measure  $D(\cdot)$ .
- Each FCG graph was first entered a graph-segmentation algorithm and functionally-coupled sites were grouped into mutually exclusive clusters. The induced grouping was then treated as one alternative representation that could be used in our contrast function. Having all the clusterings available (30 - tuple), we measured the contrast of control condition against the cognitive tasks using equation (1), with  $D(\cdot)$  denoting the Variational Information (VI) metric.



# Optimization of parameters for NI and PLI measures

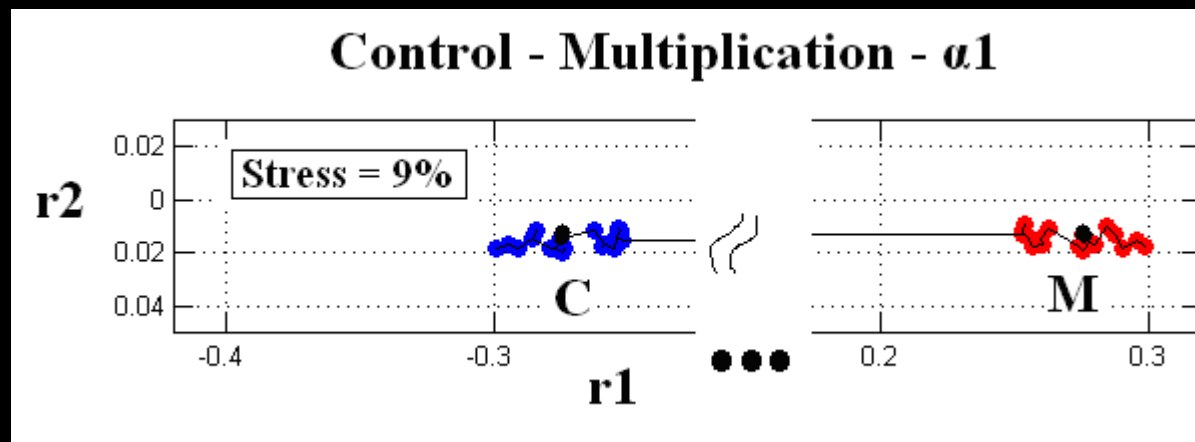
- NI (time lag, embedding dimension)  
(Nearest neighbors = 10, Theiler correction = 50, Quiroga et al., 2002)
- PLI ( $\delta_j$ ) (Lachaux et al., 1999)
- Graph segmentation (30 – tuple e.g. [1 2 2 1 .. 3 2] ) (Pavan and Pelillo, 2007) + VI (Meila, 2007)





# Visual Data Mining (VDM)

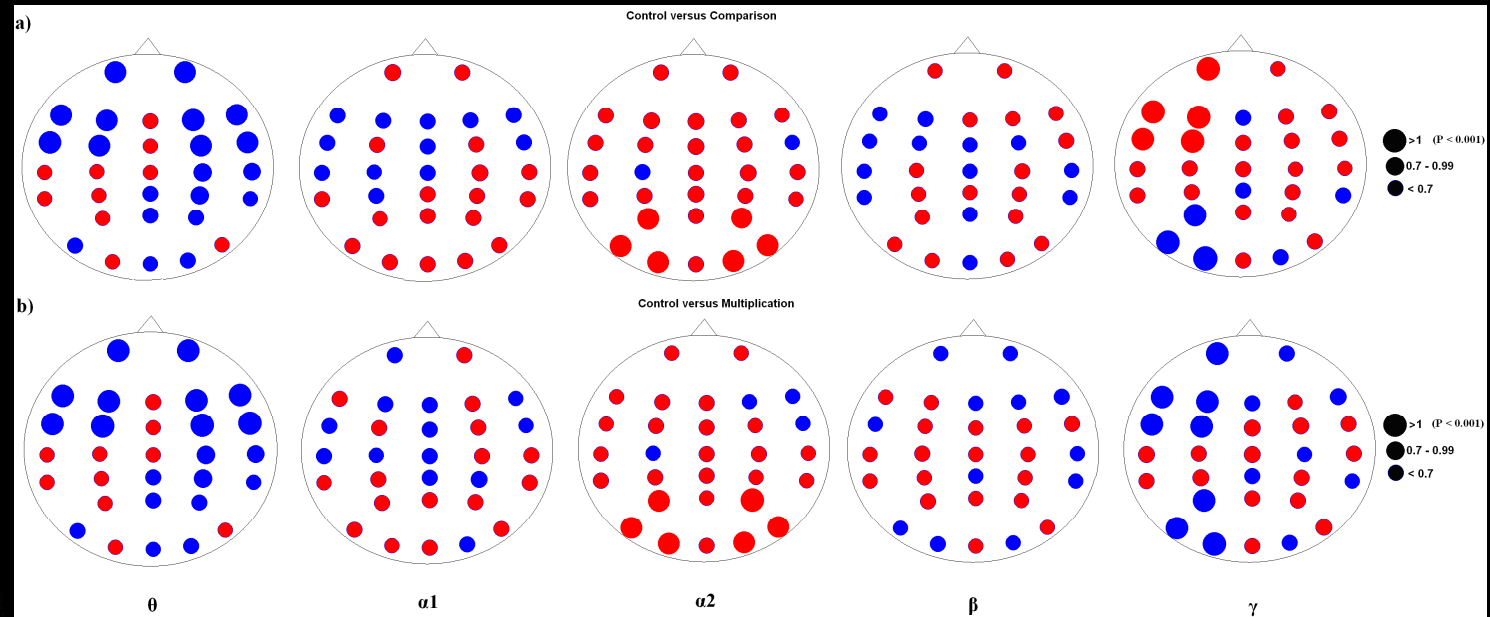
- The 30-tuple resulting from the clustering of **FCG**.
  - i) First, a representation resulted in high J-value (and hence describing well the task-related changes) was identified.
  - ii) A corresponding  $[2.N \times 2.N]$  dissimilarity matrix was then formed. This included all pairwise comparisons (through the VI metric) between the 2.N clusterings, with  $N=18$  corresponding to the number of subjects used in our study.
  - iii) The dissimilarity matrix was fed in a *multidimensional scaling* (MDS) procedure, that provided a 2D representation in which the two contrasted-sets (the N clusterings for control vs the N clusterings for a cognitive task) appeared as point-clouds of different color.
  - iv) The *Minimal Spanning Tree* (MST) Graph was finally built for the overall point-set and used to select representative nodes from each point cloud.



# Results

## Signal Power -based electrode ranking

- Topography of task-related changes in signal power



# Results

## Signal Power -based electrode ranking

- **Table 1.** Contrast-function J using multisite signal-power representation (30D vectors) – Euclidean distance

| Frequency bands | Control-Comparison | Control-Multiplication |
|-----------------|--------------------|------------------------|
| $\theta$        | 0.5665             | 0.5764                 |
| $\alpha_1$      | 0.5545             | 0.5234                 |
| $\alpha_2$      | 0.5345             | 0.5674                 |
| $\beta$         | 0.5673             | 0.5843                 |
| $\gamma$        | 0.5731             | 0.5634                 |





# Results

## Signal Power -based electrode ranking

- Table 2. Contrast-function J using reduced resolution signal-power representation (8D vectors) – Euclidean distance

| Frequency bands | Control-Comparison | Control-Multiplication |
|-----------------|--------------------|------------------------|
| $\theta$        | 0.6865             | 0.7064                 |
| $\alpha_1$      | 0.7545             | 0.5234                 |
| $\alpha_2$      | 0.8145             | 0.5674                 |
| $\beta$         | <b>0.9573</b>      | 0.8843                 |
| $\gamma$        | 0.8931             | 0.7634                 |



# Results

## Signal Power -based electrode ranking

- **Table 2b.** Contrast-function J using 2D-representation (SP-values for left and right hemisphere) – Euclidean distance

|            | Control-Comparison | Control-Multiplication |
|------------|--------------------|------------------------|
| $\theta$   | 0.5661             | 0.6136                 |
| $\alpha_1$ | 0.5261             | 0.5271                 |
| $\alpha_2$ | 0.5436             | 0.5222                 |
| $\beta$    | 0.5169             | 0.5007                 |
| $\gamma$   | 0.5226             | 0.5243                 |



# Results: Functional Connectivity Graph (FCG) representation

- Functional Connectivity Graph (FCG) representation (Frobenius norm)

| <b>**P&lt;0.001</b><br><b>* P&lt;0.01</b> | Control-Comparison |        |            | Control-Multiplication |        |            |
|---|--------------------|--------|------------|------------------------|--------|------------|
|   | <u>COH</u>         | NI     | <u>PLI</u> | <u>COH</u>             | NI     | <u>PLI</u> |
| $\theta$                                  | 1.0589             | 1.0632 | 1.0789     | 1.1113                 | 1.1252 | 1.1432     |
| $\alpha_1$                                | 1.0685             | 1.0455 | 1.0645     | 1.0371                 | 1.0579 | 1.0678     |
| $\alpha_2$                                | 1.0280             | 1.0478 | 1.0345     | 1.0433                 | 1.0619 | 1.0723     |
| $\beta$                                   | 1.0409             | 1.0266 | 1.0324     | 1.0231                 | 1.0157 | 1.0342     |
| $\gamma$                                  | 1.0189             | 1.0213 | 1.0465     | 1.0249                 | 1.0317 | 1.0456     |



# Results:Functional Connectivity Graph (FCG) representation

- Table 4. Contrast-function J for connectivity patterns after spatial grouping (lower resolution :[8x8] ) (Frobenius norm)

| <b>**P&lt;0.001</b><br><b>* P&lt;0.01</b> | Control-Comparison |          |                 | Control-Multiplication |          |                 |
|---|--------------------|----------|-----------------|------------------------|----------|-----------------|
|   | <u>COH</u>         | NI       | <u>PLI</u>      | <u>COH</u>             | NI       | <u>PLI</u>      |
| $\theta$                                  | 1.1867             | 1.2256*  | <b>1.2589**</b> | 1.2143                 | 1.2321** | <b>1.2812**</b> |
| $\alpha_1$                                | 1.2345             | 1.2445   | 1.2657          | 1.2621                 | 1.2843   | 1.3123          |
| $\alpha_2$                                | 1.2056             | 1.2121*  | <b>1.2543**</b> | 1.1931                 | 1.2023** | <b>1.2778**</b> |
| $\beta$                                   | 1.2442*            | 1.2745** | <b>1.3186**</b> | 1.2642*                | 1.2723** | <b>1.3243**</b> |
| $\gamma$                                  | 1.2134             | 1.2345   | 1.2745          | 1.2012                 | 1.2231   | 1.2545          |



# Results: Functional Connectivity Graph (FCG) representation

- Table 5. Contrast-function J for functional connectivity patterns after graph-segmentation. (VI distance)

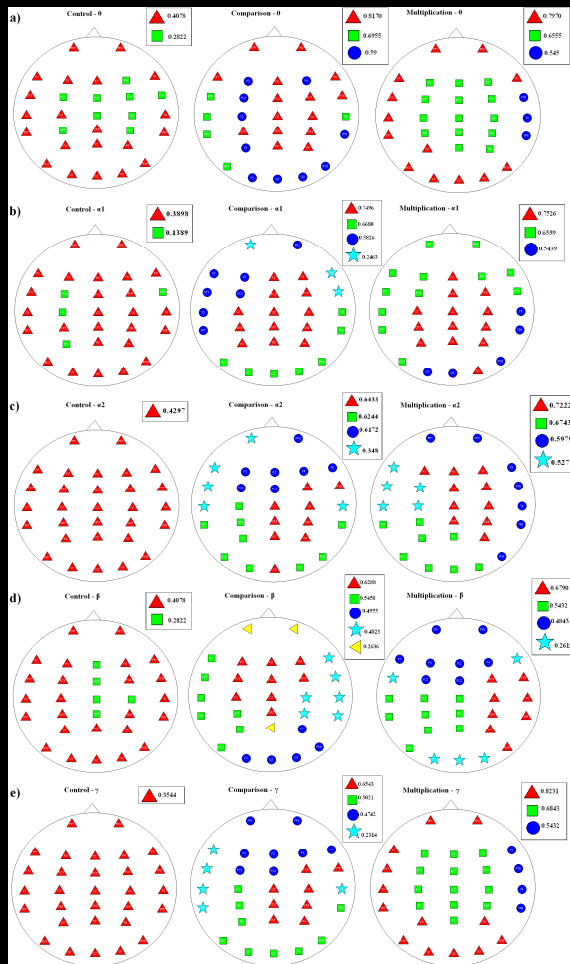
| <b>**P&lt;0.001</b><br><b>* P&lt;0.01</b> | Control-Comparison |          |            | Control-Multiplication |          |            |
|---|--------------------|----------|------------|------------------------|----------|------------|
|   | <u>COH</u>         | NI       | <u>PLI</u> | <u>COH</u>             | NI       | <u>PLI</u> |
| $\theta$                                  | 2.9067             | 3.0512** | 3.7894**   | 3.0455                 | 3.1567*  | 3.7574**   |
| $\alpha_1$                                | 2.7231             | 2.8345*  | 3.8831**   | 2.8534                 | 3.1045** | 3.8211**   |
| $\alpha_2$                                | 2.9932             | 3.0534** | 4.2484**   | 2.9245                 | 2.9234*  | 4.2578**   |
| $\beta$                                   | 2.9267             | 3.1023*  | 4.4427**   | 3.1023                 | 3.1789** | 4.2773**   |
| $\gamma$                                  | 3.0167*            | 3.1345** | 4.2085**   | 3.054*                 | 3.1034** | 3.7754**   |





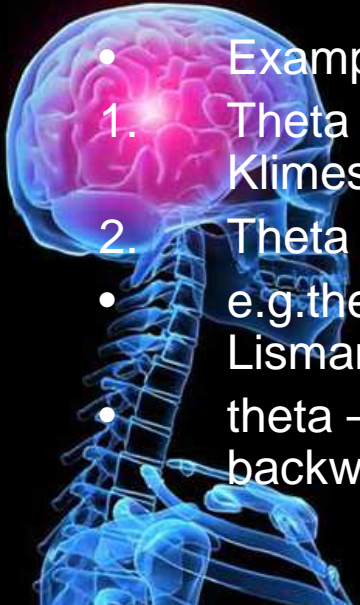
# Results: Functional-segregation prototypes

- Since the segmentation of PLI-based FCGs resulted in the most promising representation (high J, while  $P < 0.001$ ) for all frequency-bands, we've adopted the corresponding partitions better portraying the related task induced changes.

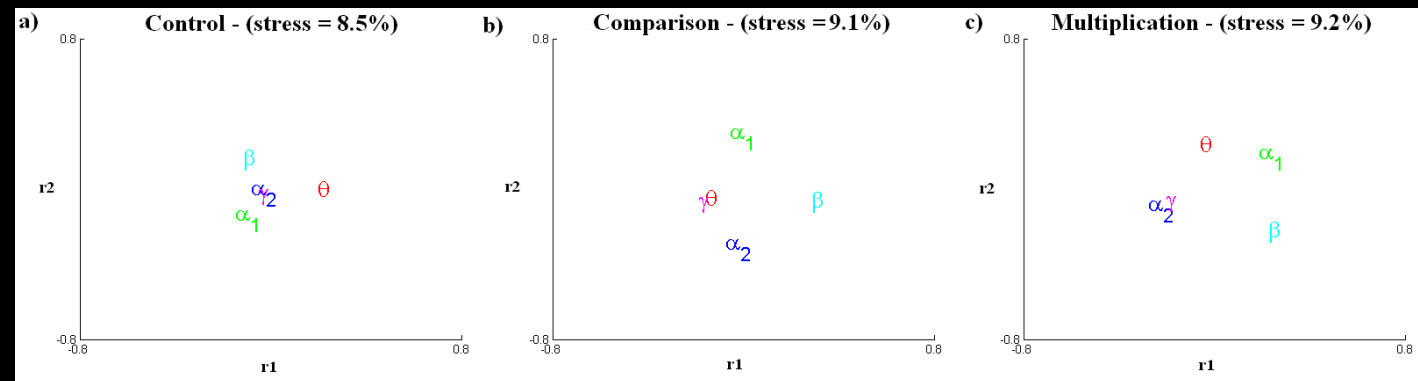
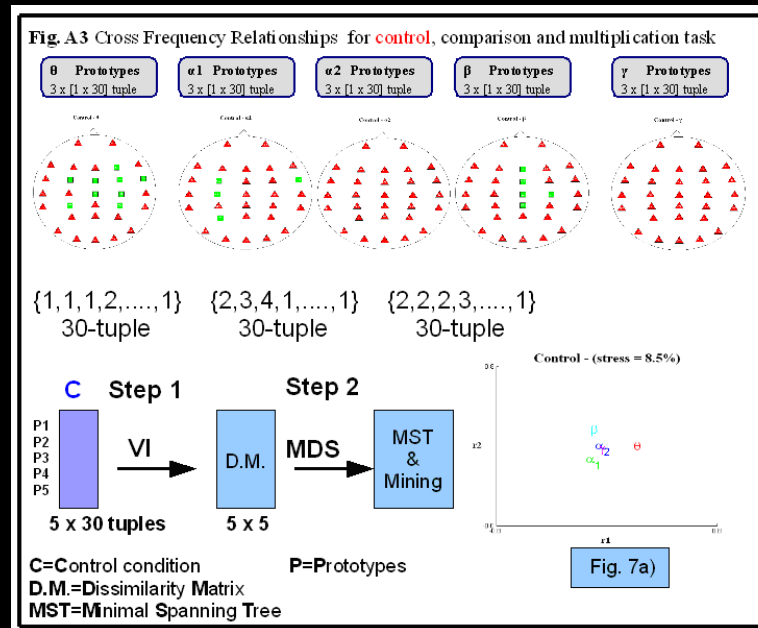


# Exploring Cross-Frequency relations based on the prototypical segregations

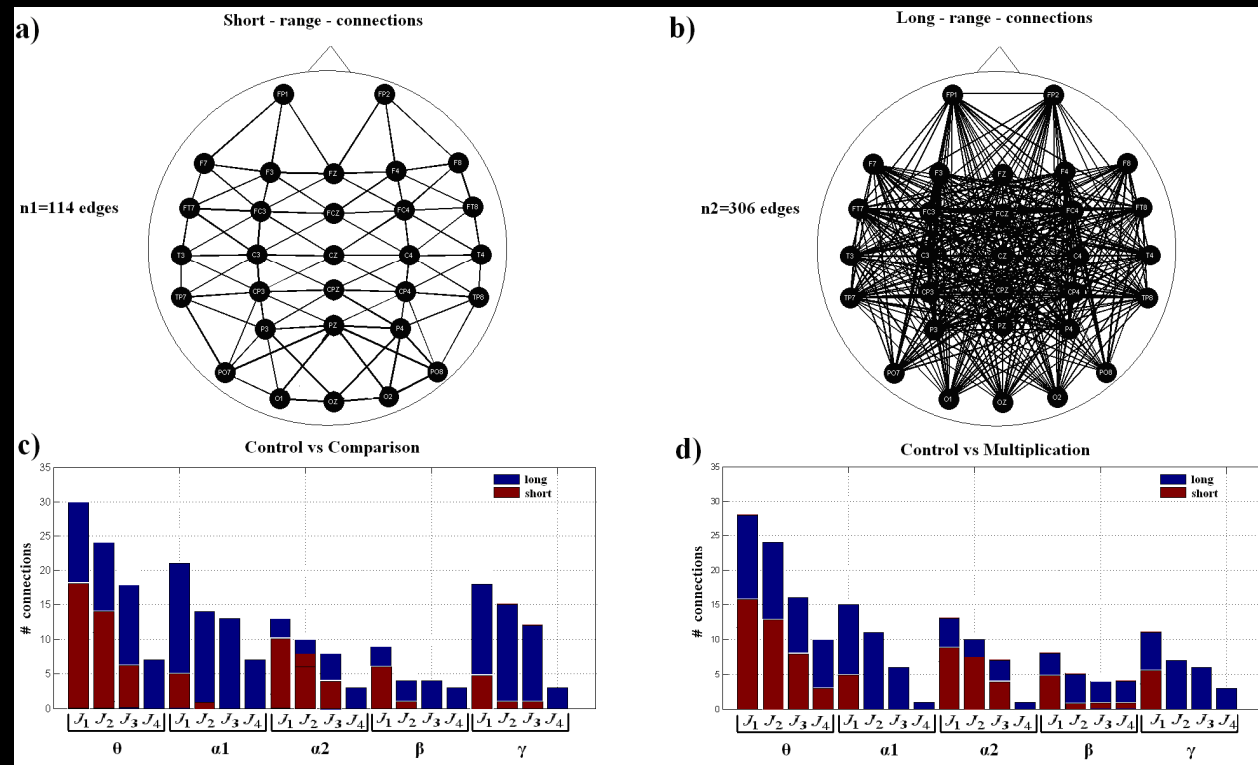
- When we assume that different cognitive systems, such as working memory, long-term memory, attention, perception and so on are related to neuronal networks of different size and distribution then it should be clear that interaction of such systems need to be reflected by coupling between the underlying neural networks.
- Different kinds of phase interaction between frequencies:
  1. Instantaneous phase of a slower oscillation modulates the amplitude of a higher frequency (Lakatos et al., 2005).
  2. Phase interactions between different frequencies called cross-frequency phase synchronization (Palva et al., 2005, Schack et al., 2002,2005).

- 
- Examples of cross-frequency interplays between cognitive systems
    1. Theta – upper alpha (working memory – long-term memory retrieval, Klimesch et al., 1997)
    2. Theta – higher frequencies (beta or gamma) during working memory
  - e.g. theta – gamma (working – short term memory processes Jensen and Lisman, 1996, 1998, 2005).
  - theta – beta (in patients suffering in neurogenic pain during a counting backward task, Sarnthein et al., 2005)

# Exploring Cross-Frequency relations based on the prototypical segregations

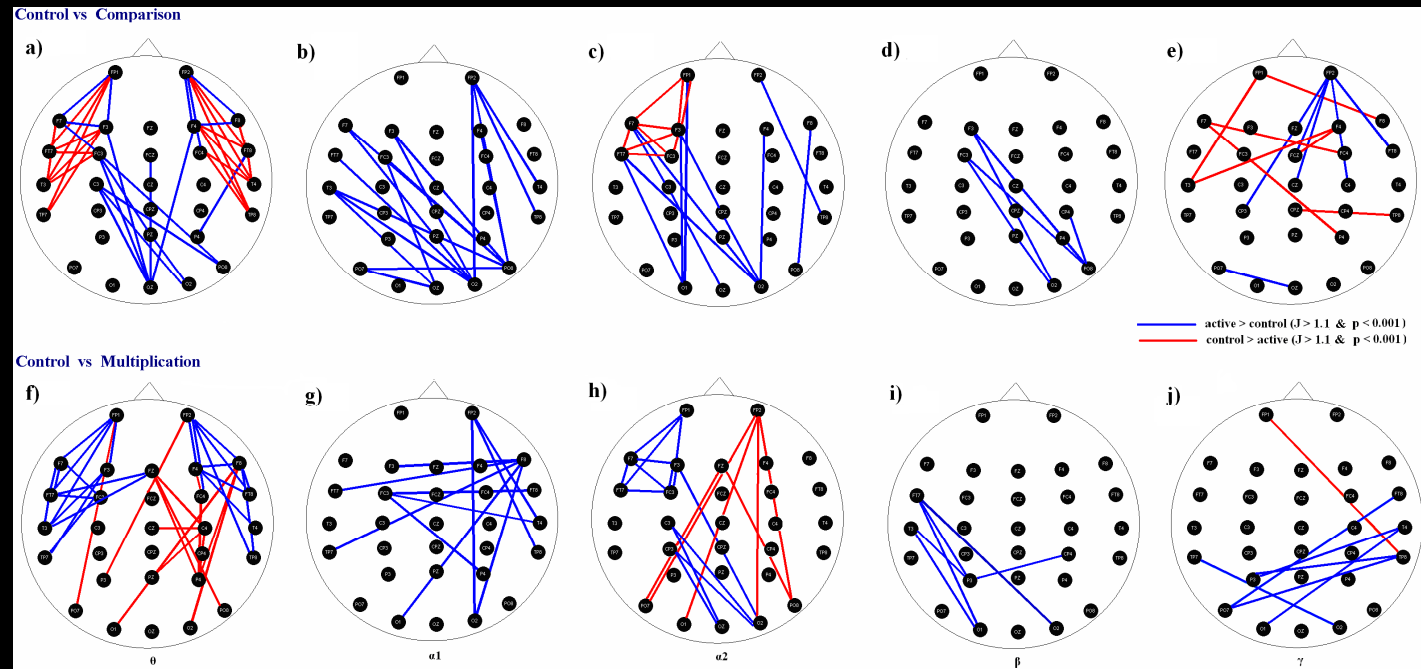


# Network Analysis : Short vs Long Range Phase-Synchrony



# Network Analysis : Short vs Long Range Phase-Synchrony

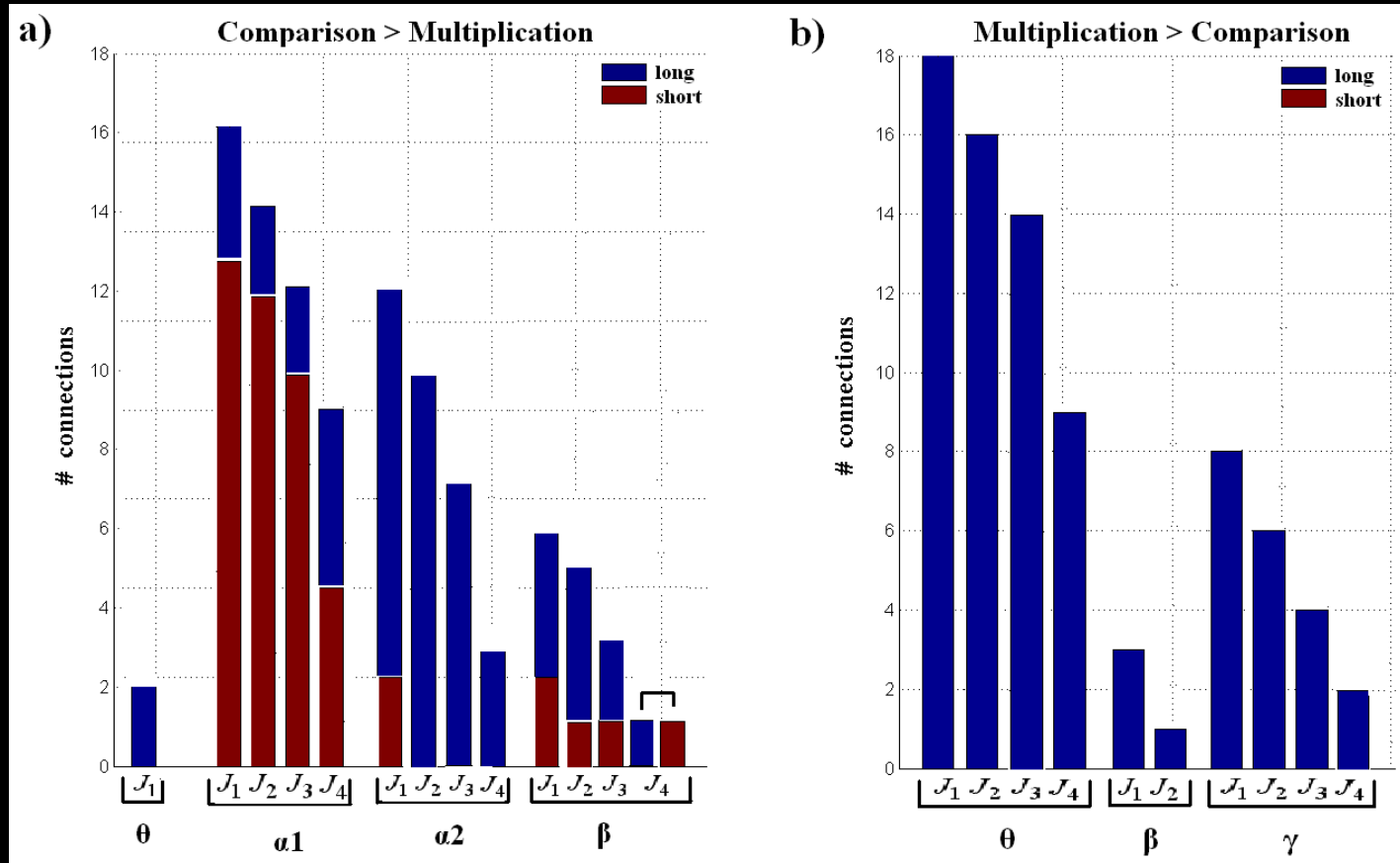
- Topographic representation of important changes (increases or decreases) in phase-synchrony, during mental calculations. Blue / red lines correspond to increased/decreased phase locking.





# Network Analysis : Short vs Long Range Phase-Synchrony

- By direct comparing the two mathematical tasks



# Mental effort in numbers

1. > 250 neuroscience papers (neurophysiology, neuropsychology)
  - aging, acalculia, dyscalculia, gender differences
2. > 200 methodological – technical papers
  - graph theory + network analysis
  - dimensionality reduction techniques (e.g MDS, ISOMAP)
  - artifact rejection techniques (e.g. ICA)
  - synchronization measures
3. 6 science books (graph theory, brain dynamics, eeg signal processing, neurophysiology, neuropsychology)
4. > 70 matlab functions (3 basic functions were translated in C)
5. > 2500 hours



Thank you for your attention !!!

